ORIGINAL RESEARCH

Seasonal primary production at the EPEA station, southwestern Atlantic: relationships with phytoplankton composition and environmental properties

Valeria Segura[1, *], Daniela Del Valle[1, 2], Vivian A. Lutz[1, 2], Moira Luz Clara[1, 2], Ricardo I. Silva[1], Jorge Fernández Acuña[1], M. Guillermina Ruiz[1], Lucrecia Allega[1], Carla F. Berghoff[1], Guillermina García Facal[1] and Lucia Epherra[1, 2]

[1]Instituto Nacional de Investigación y Desarrollo Pesquero (INIDEP), Paseo Victoria Ocampo Nº 1, Escollera Norte, B7602HSA - Mar Del Plata, Argentina. [2]Consejo Nacional de Investigaciones Científicas y Técnicas (CONICET), Argentina.
ORCID *Valeria Segura* https://orcid.org/0000-0002-0802-8070, *Daniela Del Valle* https://orcid.org/0009-0005-4137-9285, *Vivian A. Lutz* https://orcid.org/0000-0003-0951-2654, *Moira Luz Clara* https://orcid.org/0000-0002-7539-5292, *Jorge Fernández Acuña* https://orcid.org/0009-0002-7588-3154, *M. Guillermina Ruiz* https://orcid.org/0000-0003-0242-4846, *Lucrecia Allega* https://orcid.org/0000-0002-7580-392X, *Carla F. Berghoff* https://orcid.org/0009-0000-7331-8595, *Guillermina García Facal* https://orcid.org/0009-0001-3598-8464

Marine and Fishery Sciences MAFIS

ABSTRACT. This study presents the first estimates of primary production (PP) from the Marine Ecological Time Series, Estación Permanente de Estudios Ambientales (EPEA) in the Argentine Sea and examines its relationship with phytoplankton community composition and environmental factors using data obtained between 2006 and 2019. Our findings indicate that PP at EPEA exhibits seasonal pulses, with an estimated annual average of 202 ± 115 g C m^{-2} yr^{-1}, classifying the system as mesotrophic. The peak of PP occurred in spring associated with increased irradiance and water column stratification, and the dominance of diatoms, dinoflagellates, and haptophytes. Winter was the least productive season, characterized by low light levels and a deep mixed layer, with a prevalence of cryptophytes and ultraphytoplankton. In summer, PP was lower than in spring, and the community was dominated by picoplanktonic *Synechococcus* spp., adapted to low nutrients and high light. In autumn, PP increased relative to summer, associated with higher microphytoplankton biomass. A key finding was the decoupling between PP and total carbon biomass, highlighted by the high variability of the B_C to $Chla_S$ ($B_C/Chla_S$) ratio. This ratio is crucial for linking carbon-based biogeochemical models with satellite-based PP models. Deviations from the expected seasonal patterns could point to the sensitivity of coastal PP to large-scale climate influences, such as the Southern Annular Mode (SAM) and the El Niño-Southern Oscillation (ENSO). Our results evidence the physiological adaptability of phytoplankton in this dynamic coastal environment, and highlight the necessity of high-frequency sampling to improve primary productivity models in this under-sampled region.

Key words: Photosynthesis, physiological parameters, bio-optical properties, phytoplankton taxonomy, Marine Ecological Time Series.

*Correspondence:
vsegura@inidep.edu.ar

Received: 27 August 2025
Accepted: 4 November 2025

ISSN 2683-7595 (print)
ISSN 2683-7951 (online)

https://ojs.inidep.edu.ar

Journal of the Instituto Nacional de Investigación y Desarrollo Pesquero (INIDEP)

Producción primaria estacional en la estación EPEA, Atlántico Sudoccidental: relaciones con la composición del fitoplancton y las propiedades ambientales

RESUMEN. Este estudio presenta las primeras estimaciones de producción primaria (PP) de la Serie Temporal Ecológica Marina de la Estación Permanente de Estudios Ambientales (EPEA) en el Mar Argentino, y examina su relación con la composición de la comunidad fitoplanctónica y factores ambientales, utilizando datos obtenidos entre 2006 y 2019. Nuestros hallazgos indican que la PP en la EPEA presenta pulsos estacionales, con un promedio anual estimado de 202 ± 115 g C m^{-2} $año^{-1}$, lo que clasifica al sistema como mesotrófico. El pico de PP se registró en primavera, asociado a un

aumento de la irradiancia y la estratificación de la columna de agua, y al predominio de diatomeas, dinoflagelados y haptofitas. El invierno fue la estación menos productiva, caracterizada por bajos niveles de luz y una capa de mezcla profunda, con prevalencia de criptofitas y ultrafitoplancton. En verano, la PP fue menor que en primavera, y la comunidad estuvo dominada por especies picoplanctónicas de *Synechococcus* spp., adaptadas a bajos nutrientes y alta luminosidad. En otoño, la PP aumentó con respecto al verano, asociada a una mayor biomasa de microfitoplancton. Un hallazgo clave fue la disociación entre la PP y la biomasa total de carbono, evidenciada por la alta variabilidad de la relación B_C a $Chla_S$ ($B_C/Chla_S$). Esta relación es crucial para vincular los modelos biogeoquímicos basados en carbono con los modelos de PP basados en satélite. Las desviaciones de los patrones estacionales esperados podrían indicar la sensibilidad de la PP costera a las influencias climáticas a gran escala, como el Modo Anular del Sur (SAM) y El Niño-Oscilación del Sur (ENSO). Nuestros resultados evidencian la adaptabilidad fisiológica del fitoplancton en este dinámico entorno costero y resaltan la necesidad de un muestreo de alta frecuencia para mejorar los modelos de productividad primaria en esta región poco estudiada.

Palabras clave: Fotosíntesis, parámetros fisiológicos, propiedades bio-ópticas, taxonomía del fitoplancton, Series Temporales Ecológicas Marinas.

INTRODUCTION

Primary production (PP) is the process by which photosynthetic organisms, using mainly water, carbon dioxide (CO_2), and solar radiation as an energy source, produce organic matter and oxygen (O_2). In the oceans, this process is primarily carried out by phytoplankton. These organisms provide important ecosystem services by supporting higher trophic levels and regulating climate on Earth (Falkowski 2002; Falkowski et al. 2003), reducing the impact of global change through carbon assimilation and subsequent export to the deeper ocean layers as organic carbon, where a fraction of it can be sequestered in sediments (Volk and Hoffert 1985; Falkowski 2012). Global primary production by phytoplankton, as computed using a satellite model, varied from 48.7 to 52.5 Gt C y^{-1} between 1998 and 2018 (Kulk et al. 2020). Light is one of the main factors regulating primary production; therefore, models commonly rely on Photosynthesis versus Irradiance (P-E) curves, which describe the functional response of photosynthetic activity by phytoplankton to available light (Platt and Sathyendranath 1988). The most commonly used models for estimating primary production require information on the vertical distribution of chlorophyll *a* concentration (*Chla*, a proxy for phytoplankton biomass), photosynthetically active radiation (PAR) at the sea surface, its attenuation in the water column, and photosynthetic parameters (Platt and Gallegos 1980; Platt et al. 1980). The primary photosynthetic parameters, including the initial slope of the P-E curve (α) and the maximum photosynthetic rate (P_m), vary significantly among different species, and physiological states of phytoplankton. This variability directly influences a cell's light-harvesting and carbon fixation efficiency. Key factors such as cell size, pigment composition, and photoacclimation status modulate the bio-optical characteristics of the phytoplankton, which in turn dictate their light absorption capacity and ultimately their photosynthetic performance (Sathyendranath et al. 1987). As a result, phytoplankton exhibit substantial spatial and temporal variability in their photosynthetic parameters (Platt et al. 1992). In addition to species-specific traits, environmental conditions such as temperature (Bouman et al. 2005), and nutrient (Platt et al. 1992) and light availability (Falkowski 1980), also strongly influence these parameters.

Despite the ecological importance of these photosynthetic parameters for understanding and modeling primary production, *in situ* measurements remain limited, with most data collection concentrated in the North Atlantic (Kulk et al. 2020). This lack of global coverage contributes to low confidence in satellite-based estimates of marine primary production trends, highlighting the need for more thorough validation using field observations (IPCC 2019; Sathyendranath et al. 2020).

The Argentine continental shelf (ca. 34° S-55° S) is among the most productive regions of the

world's oceans, as indicated by global estimates of primary production (e.g. Longhurst et al. 1995). A primary production model estimated an annual value of 0.17 Gt for the continental shelf (Dogliotti et al. 2014), with the highest productivity occurring in frontal zones such as the shelf-break and Grande Bay (Lutz et al. 2010; Segura et al. 2013). These regions also support a highly diverse phytoplankton community, characterized by species with similar cell sizes but distinct bio-optical and photosynthetic properties (Segura et al. 2013). This high phytoplankton productivity supports the region's highly productive fisheries.

Long-term monitoring is essential for understanding dynamic ecosystems. Marine Ecological Time Series (METS) are valuable tools for characterizing seasonal and interannual variations in oceanographic, bio-optical, and biogeochemical properties, as well as assessing their links to global change. Additionally, METS help elucidate planktonic trophic structures and detect extraordinary events (Edwards et al. 2010; Valdés and Lomas 2017). In the Southwest Atlantic, where METS are rare, the Permanent Station for Environmental Studies (EPEA for its acronym in Spanish: Estación Permanente de Estudios Ambientales), established in 2000, has been one of the first in the region (O'Brien et al. 2017). EPEA is a coastal station located approximately 27 nautical miles off the coast of Mar del Plata, Argentina, at the transition between coastal and mid-shelf waters, near the 50-meter isobath (38° 28′ S, 57° 41′ W). This region is influenced by subantarctic waters advected from the middle shelf, as well as occasional intrusions of fresher waters from the Río de la Plata estuary (Carreto et al. 1995; Guerrero and Piola 1997; Lucas et al. 2005). EPEA has provided valuable long-term data on environmental variability and ecosystem dynamics and has revealed a seasonal pattern typical of temperate regimes (Carreto et al. 2004; Lutz et al 2006; Silva et al. 2009; Ruiz et al. 2020). During winter, microphytoplankton, particularly diatoms, dominate due to favorable nutrient conditions (Silva et al. 2009) and complete mixing of the water column. These conditions are also consistent with the presence of diatoms in this period (Ruiz et al. 2025). In contrast, ultraphytoplankton dominate in summer, likely benefiting from stratified waters and higher light availability (Lutz et al. 2006; Silva et al. 2009; Ruiz et al. 2025).

This study aimed to analyze the seasonal variation in primary production at EPEA between 2006 and 2019, and to examine its relationship with phytoplankton bio-optical properties and community composition. The findings were interpreted within a broader historical environmental and bio-optical context.

MATERIALS AND METHODS

Sampling and determination of variables

A total of 23 incubation experiments (P-E curves) were conducted at EPEA station (38° 28′ S, 57° 41′ W, Figure 1) between 2006 and 2019 on board different research vessels during different seasons: summer (January-March, n = 8), autumn (April-June, n = 4), winter (July-September, n = 5), and spring (October-December, n = 6) (Table 1). Hereafter, we refer to these visits to the station as $EPEA_{PP}$, to distinguish them from visits that did not include primary production measurements.

Environmental variables

During each cruise, profiles of temperature, salinity, and *in vivo* fluorescence were recorded using a Conductivity Temperature Depth (CTD, SeaBird) system, a fluorometer (SeaBird ECO), and a fluorometer sensor (Seapoint) attached to the CTD. The collected CTD data from sea surface temperature (SST) and sea surface salinity (SSS) were processed using standard Seabird software routines, subjected to quality control, and stored in the BaRDO database (Baldoni et al. 2008). Additionally, discrete salinity samples were analyzed with an Autosal Guideline 8400B salinometer.

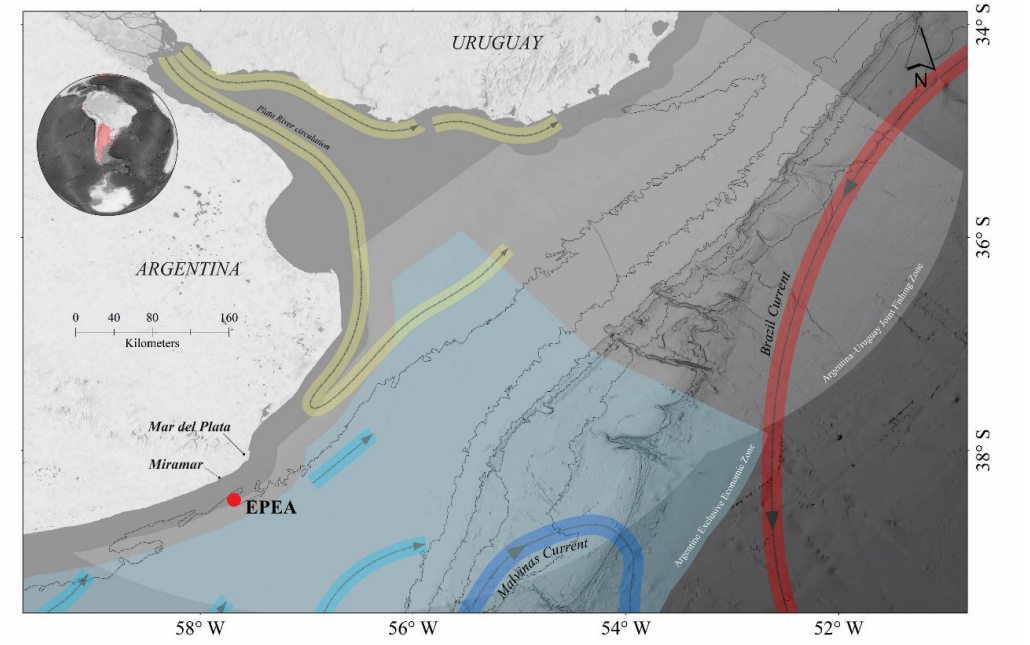

Figure 1. Location of the EPEA (Estación Permanente de Estudios Ambientales) sampling site, offshore Miramar, along with a schematic diagram of the mean circulation in the northern sector of the Argentine continental shelf. The colored lines represent the different components of this circulation: red for the Brazil Current, blue for the Malvinas Current, yellow for the mean Río de la Plata outflow, and light blue for the cold shelf waters. The white shaded area corresponds to the Argentine-Uruguayan Common Fishing Zone, while the light blue shaded area indicates the Argentine Exclusive Economic Zone. Circulation patterns were vectorized and adapted from Franco et al. (2018) and Buratti et al. (2022).

The mixed layer depth (MLD) was determined following the density criterion proposed by de Boyer Montegut et al. (2004), which defines MLD as the depth where seawater density increases by more than 0.03 kg m^{-3} relative to the density at 10 m depth. The photosynthetically active radiation (PAR: 400 to 700 nm) at the surface, E_S, was recorded continuously during the whole cruise with a cosine downwelling irradiance (LI-COR) sensor. These *in situ* measurements were then compared with daily PAR irradiance (E_{SAT}) estimated from satellite data (E_{SAT}, mol quanta m^{-2} d^{-1}) provided by NASA's Ocean Biology Processing Group (Frouin and Pinker 1995). The E_{SAT}, corresponding to the study area, was obtained from the MODIS sensor onboard the AQUA satellite and downloaded from NASA's Physical Oceanography Distributed Active Archive Center (PO.DAAC) (2019), using the 2022.0 reanalysis version (https://oceancolor.gsfc.nasa.gov/). Discrete water samples were collected (from the surface from Niskin bottles) for the subsequent determination of the macronutrients, including nitrate plus nitrite (N + N), phosphate and silicate. These nutrients were measured using Skalar SAN Plus System, with methods adapted from Armstrong et al. (1967) and Grasshoff et al. (1983) for N + N, from Murphy and Riley (1962) for phosphate, and from Grasshoff et al. (1983) for silicate. For further details on the specific analytical procedures, see Ruiz et al. (2025).

Biological variables

Additionally, seawater samples were collected at the surface and at two other selected depths for determination of biological variables described below (see Lutz et al. 2010 for more details). Details of variables, along with their corresponding symbols and units, are provided in Table 2.

Table 1. Survey data from the Estación Permanente de Estudios Ambientales where primary production (PP) was estimated ($EPEA_{PP}$). The data include the cruise name, research vessel, station ID, sampling date and time (GMT), season, and sampling depth (m) for the photosynthesis-irradiance (P-E) experiment.

Cruise	Ship	ID	Date	Hour_min	Season	P-E experiment depth
PD200602	'Puerto Deseado'	Mar2006	Mar10	4:03 pm	Summer	0
PD200603	'Puerto Deseado'	Sep2006	Sep5	10:05 pm	Spring	0
OB200803	'Oca Balda'	Nov2008	Nov20	4:36 pm	Spring	0
OB200804	'Oca Balda'	Dec2008	Dec17	2:19 pm	Spring	5
OB200901	'Oca Balda'	Jan2009	Jan21	5:53 pm	Summer	0
OB200904	'Oca Balda'	Mar2009	Mar23	2:26 pm	Summer	0
OB200906	'Oca Balda'	Apr2009	Apr29	11:19 am	Autumn	0
OB201001	'Oca Balda'	Jan2010	Jan15	10:39 pm	Summer	5
PD201005	'Puerto Deseado'	Jul2010	Jul5	5:46 pm	Winter	5
PD201008	'Puerto Deseado'	Dec2010	Dec20	10:18 pm	Spring	0
OB201103	'Oca Balda'	Feb2011	Feb26	11:45 am	Summer	5
OB201106	'Oca Balda'	Apr2011	Apr17	10:16 am	Autumn	5
PD201102	'Puerto Deseado'	Jul2011	Jul2	19:31 pm	Winter	7
PD201203	'Puerto Deseado'	Jul2012	Jul2	8:44 pm	Winter	5
OB201202	'Oca Balda'	Oct2012	Oct12	5:49 pm	Spring	5
OB201301	'Oca Balda'	Jan2013	Jan23	6:29 pm	Summer	5
OB201304	'Oca Balda'	Jul2013	Jul5	12:23 pm	Winter	5
OB201401	'Oca Balda'	Jan2014	Jan30	0:35 am	Summer	0
OB201402	'Oca Balda'	Mar2014	Mar25	8:04 pm	Summer	7.5
PD201606	'Puerto Deseado'	Nov2016	Nov7	11:04 pm	Spring	5
PD201703	'Puerto Deseado'	Jun2017	Jun2	8:53 pm	Autumn	5
VA201803	'Victor Angelescu'	Apr2018	Apr4	9:45 am	Autumn	5
VA201912	'Victor Angelescu'	Dec2019	Dec14	10:03 am	Spring	5

Chlorophyll a concentration

Total chlorophyll *a* concentration *in situ* (*Chla*) and chlorophyll *a* concentration corresponding to the phytoplankton size fraction < 5 μm ($Chla_S5$) were analyzed with a Perkin Elmer LS3 spectrofluorometer using the fluorometric method described by Holm-Hansen et al. (1965) and later modified by Lutz et al. (2010). The contribution of $Chla_S5$ to the total chlorophyll *a* concentration was determined and expressed as a percentage ($\%Chla_S5$). The integrated chlorophyll *a* concentration in the euphotic zone (Z_{EU}, here defined as the depth where the light reaches 1% of its surface value), $Chla_{ZEU}$ was calculated using the continuous *in vivo* fluorescence (Fl) profile and discrete *Chla* measurements. Depth-specific *Chla*/Fl ratios were determined and used to interpolate linearly between sampled depths, as described in Lutz et al. (2010). In cases where Fl data were not available (Jan2009 and Jan2010), a linear fit of the discrete *Chla* measurements was used to estimate $Chla_{ZEU}$.

Particulate absorption coefficients

The total particulate absorption coefficient ($a(\lambda)$) and the non-algal particle absorption coefficient ($a_{nap}(\lambda)$) were calculated using the equation pro-

Table 2. List of symbols and abbreviations used with their description and units.

Notation	Description	Units
$\%Chla_S5$	Percentage of contribution of the $Chla_S5$ to the $Chla_S$	%
^{13}C	Atom of 13 carbon	%
α	Initial slope of P-E curve	mg C h^{-1}(W m^{-2})$^{-1}$
α^B	Initial slope of P-E curve normalized by *Chla*	mg C (mg *Chla*)$^{-1}$ h^{-1}(W m^{-2})$^{-1}$
$a^B_{ph}(443)$	Specific absorption coefficient of phytoplankton at wavelength 443 nm	m^2 (mg *Chla*)$^{-1}$
$a_p(\lambda)$	Absorption coefficient of total particulate matter at wavelength λ	m^{-1}
$a_{ph}(\lambda)$	Absorption coefficient of phytoplankton at wavelength λ	m^{-1}
B_C	Biomass of total phytoplankton in terms of carbon	mg C m^{-3}
$B_C/Chla_S$	Ratio carbon biomass to chlorophyll concentration at surface	mg C (mg *Chla*)$^{-1}$
B_{Cmicro}	Biomass of microphytoplankton in terms of carbon	mg C m^{-3}
B_{Cnano}	Biomass of nanophytoplankton in terms of carbon	mg C m^{-3}
B_{Cpico}	Biomass of picophytoplankton in terms of carbon	mg C m^{-3}
B_{Cultra}	Biomass of ultraphytoplankton in terms of carbon	mg C m^{-3}
Chla	Total Chlorophyll *a* concentration *in situ*	mg m^{-3}
$Chla_S$	Total Chlorophyll *a* concentration *in situ* at the surface	mg m^{-3}
$Chla_S5$	Chlorophyll *a* concentration corresponding to the phytoplankton size fraction less than 5 μm	mg m^{-3}
$Chla_{ZEU}$	Integrated Chlorophyll *a* at the euphotic zone	mg m^{-2}
E_k	Light saturation parameter determined by the ratio P_m/α	W m^{-2}
$EPEA_{PP}$	Estación Permanente de Estudios Ambientales where primary production experiments were conducted	
E_S	Instantaneous PAR irradiance at the sea surface	μmol quanta m^{-2} s^{-1}
E_{SN}	Irradiance PAR at the sea surface at local noon	μmol quanta m^{-2} s^{-1}
E_{SAT}	Daily satellite irradiance PAR at the sea surface	mol quanta m^{-2} d^{-1}
E_Z	Irradiance PAR at depth Z	μmol quanta m^{-2} s^{-1}
Fl	*In vivo* fluorescence	relative fluorescence units
micro	Microphytoplankton class size (cells from 20 to 200 μm)	
MLD	Mixed layer depth	m
nano	Nanophytoplankton class size (cells from 5 to 20 μm)	
p	Assimilated carbon rate in each sample per hour	mg C m^{-3} h^{-1}
p_0	Surface instantaneous primary production at noon	mg C m^{-3} h^{-1}
PAR	Photosynthetically Active Radiation from 400 to 700 nm	
P^Bm	Maximum production at saturating irradiance normalized by *Chla*	mg C (mg *Chla*)$^{-1}$ h^{-1}
pico	Picophytoplankton class size (cells < 2 μm)	
P_m	Maximum production at saturating irradiance	mg C h^{-1}
PP	Primary production	
P_{ZT}	Daily primary production integrated in the water column	mg C m^{-2} d^{-1}
SSS	Surface seawater salinity	practical salinity units
SST	Surface seawater temperature	°C
ultra	Ultraphytoplankton class size (cells from 2 to 5 μm)	
Z	Depth of the station	m
Z_{EU}	Depth at which irradiance reaches 1% of the E_S	m

posed by Mitchell (1990) and the coefficients provided by Hoepffner and Sathyendranath (1992). The spectral absorption coefficient of phytoplankton ($a_{ph}(\lambda)$) was then calculated from subtraction [$a_{ph}(\lambda) = a_p(\lambda) - a_{nap}(\lambda)$] and the specific absorption coefficient of phytoplankton was obtained normalizing by *Chla* ($a^B_{ph}(\lambda)$). Details of the procedure can be found elsewhere (Ruiz et al. 2020; Lutz et al. 2021).

Phytoplankton community

To analyze the size structure of autotrophic plankton, taxa were grouped into the following categories: picophytoplankton (*pico*, < 2 μm), ultraphytoplankton (*ultra*, 2-5 μm), nanophytoplankton (*nano*, 5-20 μm) and microphytoplankton (*micro*, 20-200 μm). Identification and cell count of the *nano* and *micro* fractions were conducted using the sedimentation technique (Lund et al. 1958) and classical bibliography (Cupp 1943; Balech 1988; Tomas 1997). Taxonomic nomenclature was revised and updated following AlgaeBase (Guiry and Guiry 2025) and Nannotax3 for coccolithophores (Young et al. 2022). For the *pico* and *ultra*-fraction, epifluorescence microscopy was used, where a known volume of the sample was stained with fluorochromes; DAPI to stain the DNA, and proflavin to stain cell membranes (Booth 1993; Verity and Sieracki 1993). Morphometric measurements were performed using digitized cell images, and cell biovolumes (μm^3) were estimated based on Hillebrand et al. (1999). The total phytoplankton carbon biomass, B_C (mg C m^{-3}) and that of all size fractions (B_{Cpico}, B_{Cultra}, B_{Cnano} and B_{Cmicro}) were calculated using carbon-to-volume ratios from Menden-Deuer and Lessard (2000). Details of the procedure can be found in Karlson et al. (2010). In addition, the ratio B_C to $Chla_S$ ($B_C/Chla_S$) was calculated.

Primary production

A surface seawater sample was inoculated with a $NaH^{13}CO_3$ solution to achieve an 8% enrichment in carbon-13 and distributed into 16 square polycarbonate bottles (500 ml): 15 were incubated at an irradiance gradient, ranging approximately from 1 to 1,100 μmol quanta m^{-2} s^{-1} measured within each bottle using a scalar PAR radiometer (Model QSL-100 Biospherical Instruments) and one bottle was kept in the dark as a control. Incubations lasted 3-4 h at *in situ* seawater temperature. A non-inoculated sample was filtered onto pre-combusted Whatman GF/F glass-fiber filters at the beginning of each experiment to determine the natural ^{13}C abundance of the total particulate organic carbon pool (POC). Immediately after incubation, each bottle was filtered onto pre-combusted GF/F filters, which were stored dry on board. On land, the filters were fumed with hydrogen chloride, dried, and encapsulated for isotopic analysis (Segura 2013). The amount of POC and the percentage of ^{13}C atoms in the POC (^{13}C) on the filters were obtained using an Isotope Ratio Mass Spectrometer at the UC Davis Stable Isotope Facility (United States of America), except for samples from Nov 2006, which were analyzed by the Oceanographic Processes and Climate Laboratory of the University of Concepción (Chile). The carbon assimilation rate in each sample (p, mg C m^{-3} h^{-1}), was computed according to Hama et al. (1983), Collos and Slawyk (1985) and Fernández et al. (2005). The concentration of total dissolved inorganic carbon in the natural seawater used was 2,400 μmol L^{-1} (pers. comm. Y Collos), with a ^{13}C abundance of 1.11%. The exponential equation of Platt et al. (1980) was used to fit the P-E curve and to obtain the photosynthetic parameters: α, the slope of the P-E curve at low irradiance (mg C h^{-1} (μmol quanta m^{-2} s^{-1})$^{-1}$), and P_m, the maximum photosynthetic rate at light saturation (mg C h^{-1}). In addition, the light saturation parameter (E_k, W m^{-2}), defined as the irradiance value where the linear extrapolation of the initial slope α intersects P_m, was calculated. The parameter α was corrected for the spectral quality of the artificial light source and the phytoplankton absorption coefficient ($a_{ph}(\lambda)$) in each sample, following the methodology described by Dubinsky et al. (1986). α and P_m were normalized by $Chla_S$

at the time of sample collection to obtain α^B and P^B_m respectively.

To estimate both the surface instantaneous primary production at noon (p_0, mg C m^{-3} h^{-1}) and the daily primary production integrated in the water column (P_{ZT}, mg C m^{-2} d^{-1}), the instantaneous PAR irradiance at the sea surface (E_S), and the irradiance PAR at the depth (E_Z) were measured. The E_S were averaged into 2-hour intervals starting at 08:00 h, resulting in 9 hourly ranges per day, following Lutz et al. (2010) and Segura et al. (2021). The mean E_S between 12:00 and 14:00 h local time was defined as E_{SN} for each $EPEA_{PP}$. The E_Z was modeled using a downward attenuation coefficient (K_d) obtained from the equation of Sathyendranath and Platt (1988) accounting for the significant influence of chromophoric dissolved organic matter (CDOM), which is a major light-absorbing component in the study area (Lutz et al. 2006; Ruiz 2018). Due to gaps in our CDOM data, a monthly averaged K_d derived from historical measurements was used to calculate both E_Z and the P_{ZT}. The p_0 and P_{ZT} were calculated at each station following the parameterization of Platt et al. (1980). The following assumptions were made: $Chla_{ZEU}$ profiles remained constant throughout the day, and photosynthetic parameters were constant both with depth (Z) and over the course of a day. Details of the procedure can be found elsewhere (Segura et al. 2010, 2021).

Statistical analysis

Descriptive statistics on a total of 23 $EPEA_{PP}$ with available bio-optical ($Chla_S$, $Chla_S5$, $a^B_{ph}(\lambda)$), primary production parameters, carbon biomass of phytoplankton and environmental (E_{SN}, E_{SAT}, SST, SSS, MLD) data (Table 3) was performed using R and visualized using box plots. Data were grouped by season: summer (January-March, n = 8), autumn (April-June, n = 4), winter (July-September, n = 5), and spring (October-December, n = 6). This visualization characterized the $EPEA_{PP}$ in relation to the historical data from 2000 to 2019 providing context for their variability. To achieve this, previously published data from Ruiz et al. (2020) and Viñas et al. (2021) for 2000-2017 were integrated with new observations from 2018-2019.

Spearman's rank correlations (r_s) were calculated to assess associations between variables and parameters. The correlations were considered significant at $p < 0.05$. Principal Component Analysis (PCA) was performed using R (version 4.4.1) with the FactoMineR package (Lê et al. 2008). The analysis was based on the correlation matrix and included the Kaiser-Meyer-Olkin (KMO) index to evaluate the suitability of surface environmental variables (E_{SAT}, SST, SSS, MLD) and biological variables ($Chla_S$, $a_{ph}(443)$, p_0, B_C and $B_C/Chla_S$). This exploratory approach aimed to identify potential associations among variables within the dataset.

RESULTS

Variation in environmental properties

Irradiance

Irradiance showed high variability across the different $EPEA_{PP}$ regardless of season, with highest irradiance values, E_{SN} and E_{SAT}, recorded during summer and spring (Table 3; Figure 2 A). Although E_{SN} measurements are instantaneous and subject to high variability (e.g. due to cloud cover), they exhibited a seasonal pattern similar to that observed in the E_{SAT} data (Figure 2 A; Table 4). A significant correlation was found between E_{SN} and E_{SAT} (r_s = 0.82, $p < 0.005$, n = 23; Figure 3).

Temperature and salinity

SST during $EPEA_{PP}$ ranged from 10.37 (Sep2006) to 21.10 °C (Feb2011). It showed high variability in autumn and spring, with a range of approximately 5-6 °C within each season (Figure 2 B; Table 3). In particular, the $EPEA_{PP}$ conducted in Apr2018 (autumn) and Dec2008 (spring) presented SST values above and below in relation to the historical data from 2000 to 2019, respective-

ly. However, none of the values were detected as outliers (Figure 2 B). SSS also exhibited considerable variability across $EPEA_{PP}$, ranging from a minimum of 33.44 (Dec2008) to a maximum of 34.30 (Apr2018). Some cruises exhibited values at or below the lower first quartile of historical data, with Jul2010 being an outlier (Figure 2 C).

Mixed layer depth

The MLD during $EPEA_{PP}$ ranged from 7 m (Dec2008) to 48 m (Jul2012, i.e. homogeneous water column). High variability in MLD was observed within seasons (Table 3). On average, MLD was shallower in summer and spring, ranging from 16 to 21 m, and deeper in autumn and winter, at over 30 m during autumn and winter (Table 3). Apr2018 and Dec2019 were identified as outliers in the distribution of MLD values (Figure 2 D).

Variation in biological variables

Chlorophyll a concentration

The $Chla_S$ during the $EPEA_{PP}$ ranged from 0.33 mg m^{-3} (Jan2014) to 5.38 mg m^{-3} (Dec2008) (Table 3). In general, $Chla_S$ values were < 2.00 mg m^{-3} regardless of the period analyzed, except in spring when two outliers were identified (Dec2008 and Nov2016) (Figure 4 A). A significant negative correlation was found between $Chla_S$ and SST (r_s = -0.53, $p < 0.05$, n = 23; Figure 4 A). In the $EPEA_{PP}$, $Chla_S5$ ranged from 0.41 mg m^{-3} (Dec2010) to 2.63 mg m^{-3} (Dec2008), with outliers in Oct2012, Dec2008, and Mar2014 (Table 3; Figure 4 B). $\%Chla_S5$ ranged from 18 to 93%, with spring and winter showing the greatest variability (Table 3; Figure 4 C). $Chla_{ZEU}$ ranged from 21 (Jan2014) to 435 mg m^{-2} (Mar2006) (Table 3), with the greatest variability in spring and summer, when values spanned over an order of magnitude.

Specific phytoplankton absorption coefficient

The $a^B_{ph}(443)$ values varied by an order of magnitude during the $EPEA_{PP}$, ranging from 0.020 (Jul2013) to 0.129 m^2 (mg $Chla)^{-1}$ (Nov2016) (Table 3). In general, spring and summer $EPEA_{PP}$ were the most variable periods within the $EPEA_{PP}$ (Table 3; Figure 4 D). Significant positive correlations were observed between $a_{ph}(443)$ and $Chla_S$ (r_s = 0.75, $p < 0.05$, n = 23), $a_{ph}(443)$ and $Chla_{ZEU}$ (r_s = 0.65, $p < 0.05$, n = 23), and $a_{ph}(443)$ and $Chla_S5$ (r_s = 0.68, $p < 0.05$, n = 16) (Figure 4 D).

Phytoplankton composition

The B_C in the $EPEA_{PP}$ ranged from 10 to 110 mg C m^{-3} (Table 3; Figure 5). On average, B_C was higher in summer and autumn compared to winter and spring. During summer, B_{Cpico} accounted for, on average, more than 60% of total B_C, primarily driven by cyanobacteria of the genus *Synechococcus* Nägeli, 1849 (Figure 5). Notable exceptions occurred in Jan2010 and Mar2014, when B_C was dominated by chrysophytes and cryptophytes from B_{Cultra}, respectively (Figure 5). In autumn, B_{Cmicro} represented, on average, 44% of B_C, and was dominated by the large diatom *Trieres sinensis* (Greville, 1866) (Figure 5). In winter, cryptophytes from B_{Cultra} dominated, contributing on average more than 40% to total B_C, followed by various microplanktonic diatoms like *Eucampia* sp. Ehrenberg, 1839, which contributed ~ 30% to total B_C (Figure 5). In spring, all size fractions contributed similar average proportions to total phytoplankton B_C (Figure 5). The mean $B_C/Chla_S$ ratio varied seasonally, ranging from 15 ± 8 in winter to 89 ± 47 in summer (Table 3), and it was positively correlated with SST (r_s = 0.77, $p < 0.05$, n = 23) (Figure 3).

Photosynthesis parameters and primary production rates

Although marked variation in the shape of the P-E curves was observed across different $EPEA_{PP}$, regardless of the season (data not shown), the unnormalized photosynthetic parameters were related to each other. These variations resulted in highly variable values of photosynthetic parameters, with mean α^B varying from 0.06 ± 0.04 in summer to 0.10 ± 0.03 mg C (mg $Chla)^{-1}$ h^{-1} (W $m^{-2})^{-1}$ in

Table 3. Seasonal averages and standard deviations of physical, chemical, biological variables and phytoplankton primary production parameters (corresponding symbols, abbreviations and units in Table 2). Data are presented for Summer (Jan-Mar), Autumn (Apr-Jun), Winter (Jul-Sep), and Spring (Oct-Dec) periods across various sampling years. N indicates the number of observations for each variable in each season.

ID	E_S	E_{SAT}	SST	SSS	MLD	N + N	$Chla_S$	$Chla_{ZEU}$	$Chla_S5$	$a_{ph}(443)$	$a^B_{ph}(443)$
Summer											
Mar2006	1,214	30	18.97	33.74	14	0.96	0.72	435	-	0.03	0.04
Jan2009	1,749	66	19.98	33.47	8	-	0.35	32	-	0.02	0.06
Mar2009	835	38	20.54	33.81	30	0.19	0.83	25	0.46	0.04	0.04
Jan2010	1,614	58	19.93	33.74	9	0.36	1.12	37	-	0.06	0.05
Feb2011	903	42	21.10	33.81	27	0.34	1.11	39	0.66	0.05	0.04
Jan2013	1,362	54	20.72	33.65	8	-	1.27	41	-	0.03	0.02
Jan2014	1,511	57	20.77	33.91	11	0.65	0.33	21	-	0.03	0.10
Mar2014	1,275	40	19.17	34.26	21	1.05	1.34	36	0.99	0.05	0.04
Mean	1,308	48	20.15	33.80	16	1.05	0.88	83	0.70	0.04	0.05
sd	323	12	0.77	0.23	9	0.35	0.39	142	0.27	0.01	0.02
N	8	8	8	8	8	6	8	8	3	8	8
Autumn											
Apr2009	1,120	30	18	34.10	44	0.18	1.04	27	0.52	0.02	0.02
Apr2011	458	20	14	34.10	47	0.68	0.99	27	0.61	0.03	0.03
Jun2017	509	15	16	34.00	48	-	1.89	34	1.08	0.06	0.03
Apr2018	1,073	25	20	34.30	15	0.29	1.05	39	0.59	0.04	0.03
Mean	790	23	16.80	34.13	39	0.38	1.24	32	0.70	0.04	0.03
sd	355	6	2.65	0.13	16	0.26	0.43	6	0.26	0.02	0.01
N	4	4	4	4	4	3	4	4	4	4	4
Winter											
Sep2006	868	32	10	33.90	14	4.14	1.32	0.71	0.03	0.02	0.08
Jul2010	817	13	12	33.50	13	3.83	1.36	44	0.94	0.06	0.04
Jul2011	527	17	12	33.90	41	0.00	1.57	37	-	0.04	0.03
Jul2012	475	17	12	33.90	48	2.53	1.11	27	0.57	0.03	0.03
Jul2013	443	15	12	34.10	35	1.09	1.19	28	0.74	0.02	0.02
Mean	626	19	12	33.86	30	2.32	1.31	34	0.74	0.04	0.03
sd	201	8	0.74	0.22	15.93	1.77	0.18	8.04	0.15	0.02	0.01
N	5	5	5	5	5	5	5	5	5	5	5
Spring											
Nov2008	711	58	14	33.80	15	-	1.36	48	-	0.07	0.05
Dec2008	1,590	63	14	33.40	7	0.79	5.38	300	2.63	0.27	0.05
Dec2010	1,713	65	17	33.60	13	0.15	0.77	31	0.41	0.03	0.04
Oct2012	1,112	43	12	33.70	10	0.58	1.82	80	1.70	0.08	0.04
Nov2016	1,435	57	13	33.60	30	1.98	4.09	114	0.73	0.53	0.13
Dec2019	1,288	50	16	33.80	48	-	2.45	58	0.87	0.13	0.05
Mean	1,308	56	14	33.65	21	0.88	2.65	105	1.27	0.19	0.06
sd	362	8	2	0.15	16	0.78	1.76	100	0.90	0.19	0.03
N	6	6	6	6	6	4	6	6	5	6	6

Table 3. Continued.

ID	α^B	P^Bm	E_k	p_0	P_{ZT}	B_C	B_{Cmicro}	B_{Cnano}	B_{Cultra}	B_{Cpico}	$B_C/Chla_S$
Summer											
Mar2006	0.06	5.14	81.9	4.37	385	60.6	4.7	1.2	7.2	47.5	84
Jan2009	0.00	0.50	357.1	0.17	87.67	16.4	1.8	3.2	4.9	6.5	47
Mar2009	0.07	4.89	68.8	4.34	440.6	60.8	13.6	2.2	5.0	39.9	74
Jan2010	0.03	1.55	56.5	1.74	342.8	108.5	2.5	20.8	50.2	35.0	97
Feb2011	0.04	2.01	49.0	2.18	356.4	110.5	1.5	1.7	9.2	98.1	100
Jan2013	0.04	1.49	38.1	1.88	392.2	56.0	1.5	13.5	5.3	35.7	44
Jan2014	0.11	1.72	15.8	0.56	261.1	59.5	5.4	2.7	3.9	47.4	181
Mar2014	0.10	4.69	45.6	6.26	964.6	45.6	2.1	2.3	22.3	18.8	34
Mean	0.06	2.75	89.1	2.69	403.8	64.7	4.2	6.0	13.5	41.1	83
sd	0.04	1.84	110.1	2.10	251.5	31.3	4.1	7.2	16.0	27.0	47
N	8	8	8	8	8	8	8	8	8	8	8
Autumn											
Apr2009	0.09	4.11	45.7	4.26	493	81.2	57.6	6.9	9.1	7.6	78
Apr2011	0.07	2.16	30.9	2.30	231	48.6	23.6	4.8	15.7	4.5	49
Jun2017	0.08	2.81	35.1	5.11	298	40.3	3.6	4.7	27.7	4.3	21
Apr2018	0.06	1.43	23.8	1.60	302	49.1	22.8	11.4	14.6	0.4	47
Mean	0.08	2.63	33.9	3.32	331	54.8	26.9	7.0	16.8	4.2	49
sd	0.01	1.14	9.1	1.64	112.8	18.1	22.5	3.1	7.8	3.0	23
N	4	4	4	4	4	4	4	4	4	4	4
Winter											
Sep2006	0.87	10.9	1.15	265.1	19.9	11.8	3.6	1.9	2.6	15	-
Jul2010	0.09	3.43	38.1	4.60	501	19.9	8.3	1.0	8.7	1.9	15
Jul2011	0.08	1.32	16.5	2.06	205	12.1	0.5	0.4	8.3	2.9	8
Jul2012	0.16	1.79	11.2	1.99	242	10.4	3.2	1.5	4.2	1.5	9
Jul2013	0.10	1.91	19.1	2.25	213	32.0	4.2	2.2	20.7	4.8	27
Mean	0.10	1.86	19.2	2.41	285.2	18.9	5.6	1.8	8.8	2.7	15
sd	0.03	0.97	11.2	1.30	123	8.6	4.5	1.2	7.3	1.3	7.56
N	5	5	5	5	5	5	5	5	5	5	5
Spring											
Nov2008	0.04	4.05	101.3	4.44	600	21.2	5.8	4.6	3.8	7.0	16
Dec2008	0.08	3.61	45.1	19.39	2,418	86.3	27.5	29.2	13.5	16.1	16
Dec2010	0.03	2.52	84.0	1.90	336	24.8	1.8	4.6	6.7	11.5	32
Oct2012	0.09	2.76	30.7	5.02	1,156	47.1	1.7	5.3	37.0	3.1	26
Nov2016	0.08	1.81	22.6	7.38	1,713	35.0	10.9	11.7	11.5	0.9	9
Dec2019	0.13	1.75	13.5	4.30	927	29.9	9.2	5.9	11.0	3.8	12
Mean	0.08	2.75	49.5	7.07	1,192	40.7	9.5	10.2	13.9	7.1	19
sd	0.04	0.93	35.4	6.28	765.4	24.1	9.6	9.7	11.8	5.8	9
N	6	6	6	6	6	6	6	6	6	6	6

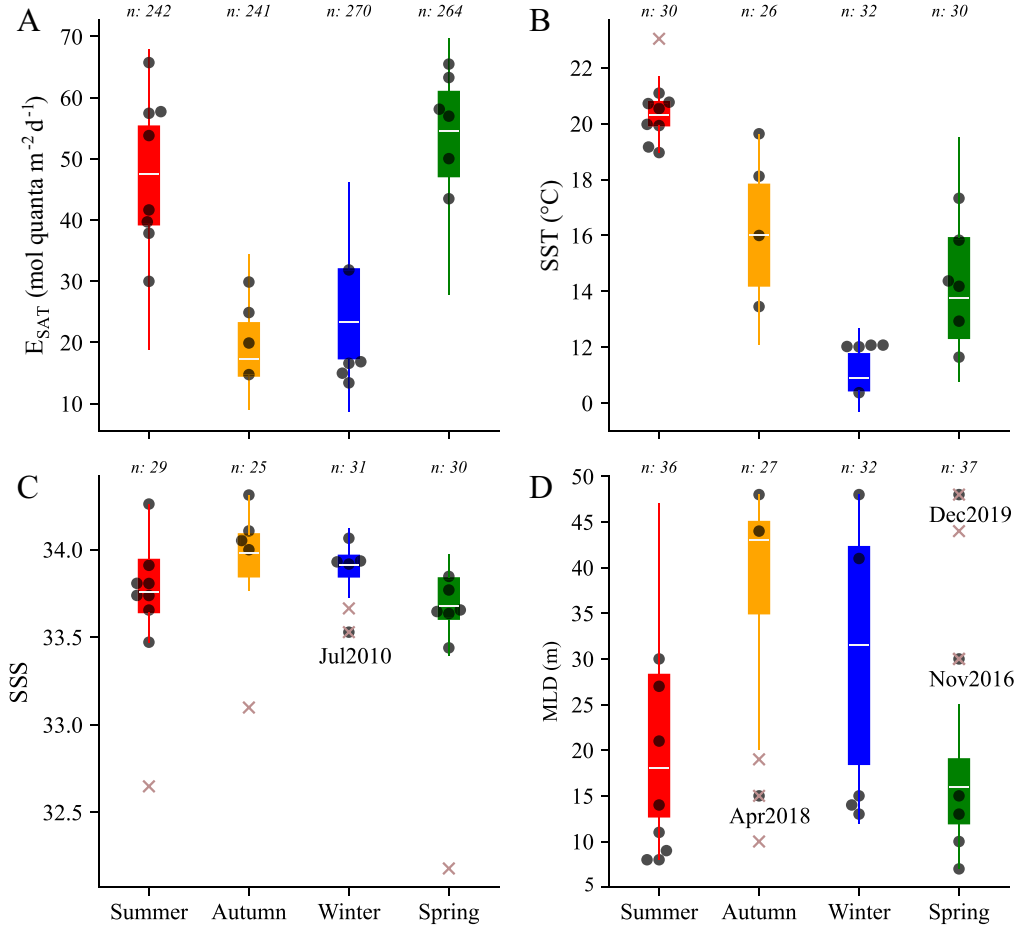

Figure 2. Box plot of E_{SAT} (A), SST (B), SSS, and MLD (D) at surface during the different seasons: summer (red), autumn (orange), winter (blue) and spring (green) in the EPEA Series from 2000 to 2019. Circles indicate the $EPEA_{PP}$ stations and crosses indicate outliers relative to the seasonal time series. The *n* represents the number of samples for period utilized.

winter. The mean seasonal P^Bm ranged from 1.86 ± 0.97 in winter to 2.75 ± 1.84 mg C (mg *Chla*)$^{-1}$ h^{-1} in summer, and E_k ranged from 19.2 ± 11.2 in winter to 89.9 ± 110 W m^{-2} in summer (Table 3). The highest values of P^Bm (> 4.50 mg C (mg *Chla*)$^{-1}$ h^{-1}) were found in Mar2006, Mar2009, Mar2014. No significant correlations were found between the normalized photosynthetic parameters (Figure 3). A significant correlation was also observed between the α^B and E_k (r_s = -0.64, $p < 0.005$, n = 23) and between the α^B and E_{SAT} (r_s = -0.42; $p < 0.005$, n = 23), SST (r_s = -0.43; $p < 0.005$, n = 23), and MLD (r_s = 0.47; $p < 0.005$, n = 23) (Figure 3).

The p_0 and P_{ZT} varied considerably in the $EPEA_{PP}$, ranging from 2.41 ± 1.30 to 7.07 ± 6.28 mg C m^{-3} h^{-1}, and from 285 ± 123 and 1,191 ± 765 mg C m^{-2} d^{-1}, respectively (Table 3). The highest values of primary production were found in spring (Dec2008 and Nov2016), while the lowest values were recorded in summer (Jan2009) (Table 3; Figure 6). However, the $p_0/Chla_S$ ratio during summer, particularly in March, reached its highest values (Figure 6). Significant correlations were found between p_0 and $Chla_S$ (r_s = 0.62, $p < 0.05$, n = 23), p_0 and P^Bm (r_s = 0.75, $p < 0.05$, n = 23); P_{ZT} and $Chla_S$ (r_s = 0.53, $p < 0.05$, n = 23), and P_{ZT} with $Chla_{ZEU}$

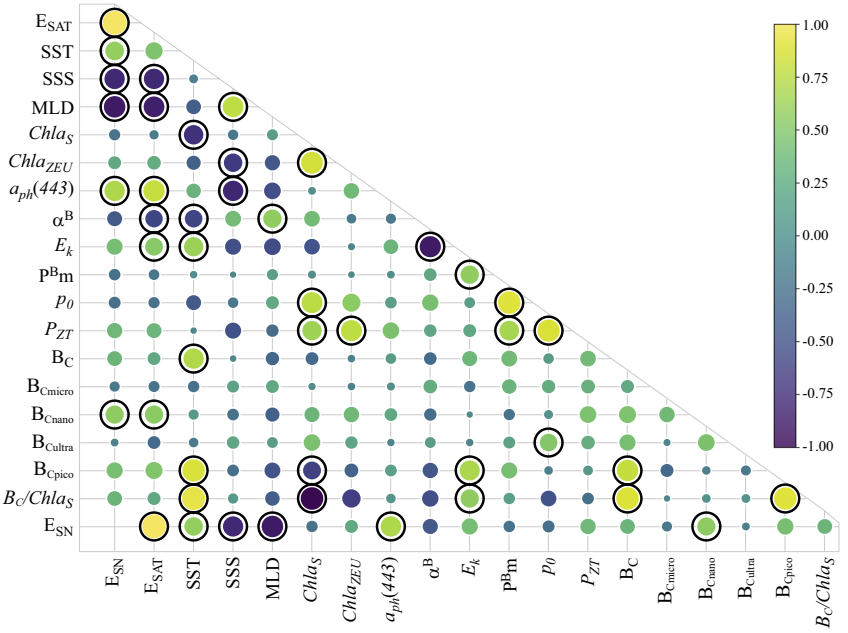

Figure 3. Spearman correlation matrix among physical (E_{SN}, E_{SAT}, MLD, SST, SSS) and biological (*Chla*$_s$, *Chla*$_{ZEU}$, $a_{ph}(443)$, α^B, P^Bm, E_k, p_0, P_{ZT}, B_C, B_{Cmicro}, B_{Cnano}, B_{Cultra}, B_{Cpico}, $B_C/Chla_S$) at surface in the $EPEA_{PP}$. Circle size and color represent the strength and sign of the correlation, from – 1 (dark purple) to + 1 (yellow), as indicated by the color scale. Circles with a black outline indicate statistically significant correlations.

($r_s = 0.56$, $p < 0.05$, $n = 23$), P_{ZT} and P^Bm ($r_s = 0.56$, $p < 0.05$, $n = 23$) (Figure 3).

Environmental and biological characterization of $EPEA_{PP}$

Principal component analysis showed that two principal components (PCs) explained 66% of the total variance of the environmental and biological properties studied in the $EPEA_{PP}$. The first component (PC1, ~ 36%) was primarily associated with biological variables such as *Chla*$_S$, $a_{ph}(443)$, and p_0 and the second component (PC2, ~ 30%) was mainly influenced by environmental variables such as E_{SAT}, SST, SSS, and MLD, as well as the biological variables B_C and the $B_C/Chla_S$ ratio (Figure 7 A). Projections of the $EPEA_{PP}$ stations on the PC_S map showed, for the summer, a negative association with PC1 and a positive one with PC2 (Figure 7 B). This suggests that these stations were characterized by a well illuminated environment, high-temperature, and stratified waters. Additionally, they were characterized by low *Chla*$_S$, low $a_{ph}(443)$, low p_0 and a high $B_C/Chla_S$ ratio. In autumn, the projections of the $EPEA_{PP}$ showed negative association with the variables from the PC1 and PC2 components (Figure 7 A). This indicates that these stations were characterized by low light availability, low SST, high SSS; and a deep MLD, low *Chla*$_S$, low $a_{ph}(443)$, low p_0, and high $B_C/Chla_S$ ratio. In winter, the $EPEA_{PP}$ exhibited a negative relationship primarily with the variables associated with PC2 (Figure 7 A). This suggests that they were characterized by a low E_{SAT}, low SST, a deep MLD and low B_C. In spring, the $EPEA_{PP}$ showed high dispersion along the PC1, and were generally positively associated with the variables of both PC1 and PC2 components (Figure 7 A). This suggests that these stations were characterized by illuminated environments with high E_{SAT}, a stratified water column with shallow MLD, high *Chla*$_S$, elevated $a_{ph}(443)$, high primary production rates and $B_C/Chla_S$ ratio (Figure 7 B).

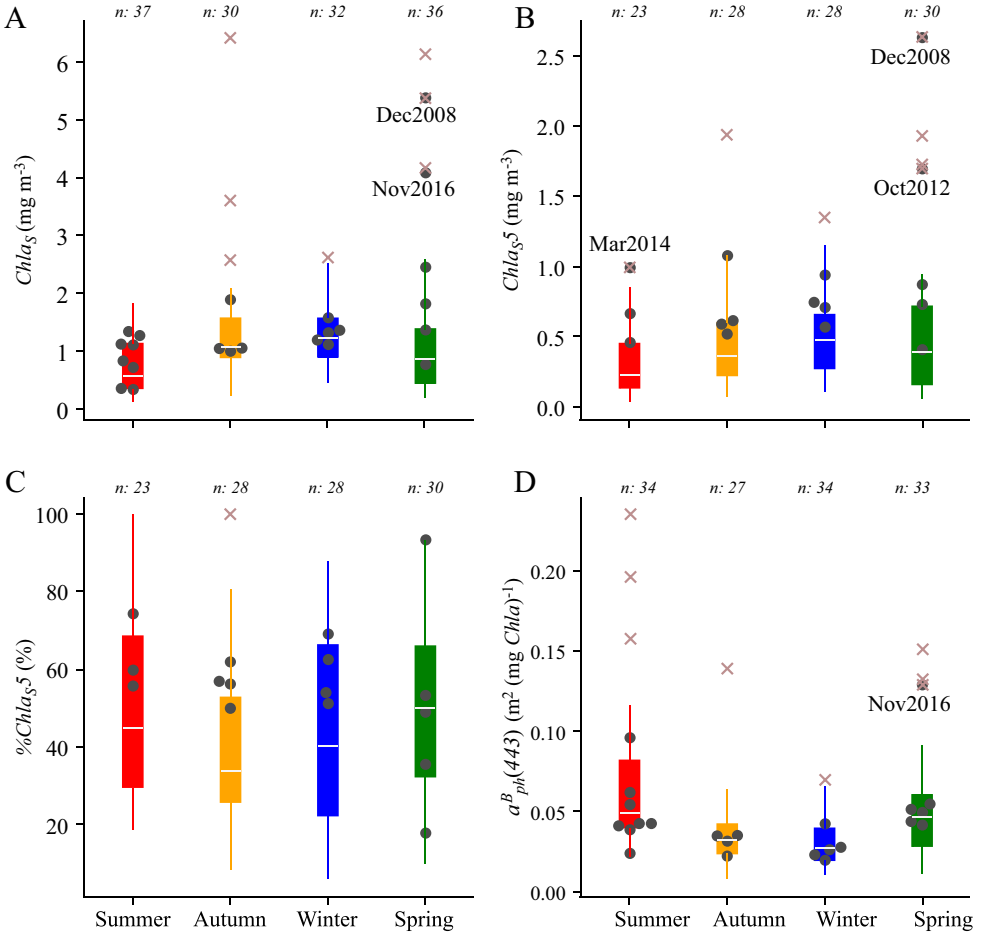

Figure 4. Box plot of $Chla_S$ (A), $Chla_S5$ (B), $\%Chla_S5$ (C), and $a^B_{ph}(443)$ (D) at surface during the different seasons: summer (red), autumn (orange), winter (blue) and spring (green) in the EPEA Series from 2000 to 2019. Circles indicate the $EPEA_{PP}$ stations and crosses indicate outliers relative to the seasonal time series. The *n* represents the number of samples for period utilized.

DISCUSSION

Phytoplankton production: efficiency and community dynamics

The sustainability of an ecosystem is determined by its ability to maintain a balance between biomass production and loss at each trophic level. To assess the carrying capacity of a system, it is necessary to know the rates of primary production and approximately half of the global PP is generated by oceanic phytoplankton (Longhurst et al. 1995). The annual PP, estimated from seasonal averages at EPEA, was 202 ± 115 g C m^{-2} yr^{-1}, which places this coastal system within the mesotrophic range (100-300 g C m^{-2} yr^{-1}), according to the classification proposed by Nixon (1995), reflecting moderate nutrient availability and primary productivity. Although estimates of PP in the Southern Hemisphere, particularly in the Southwestern Atlantic, remain limited (Lutz et al. 2018), the values obtained in this study (ranged from 88 to 2,418 mg C m^{-2} d^{-1})

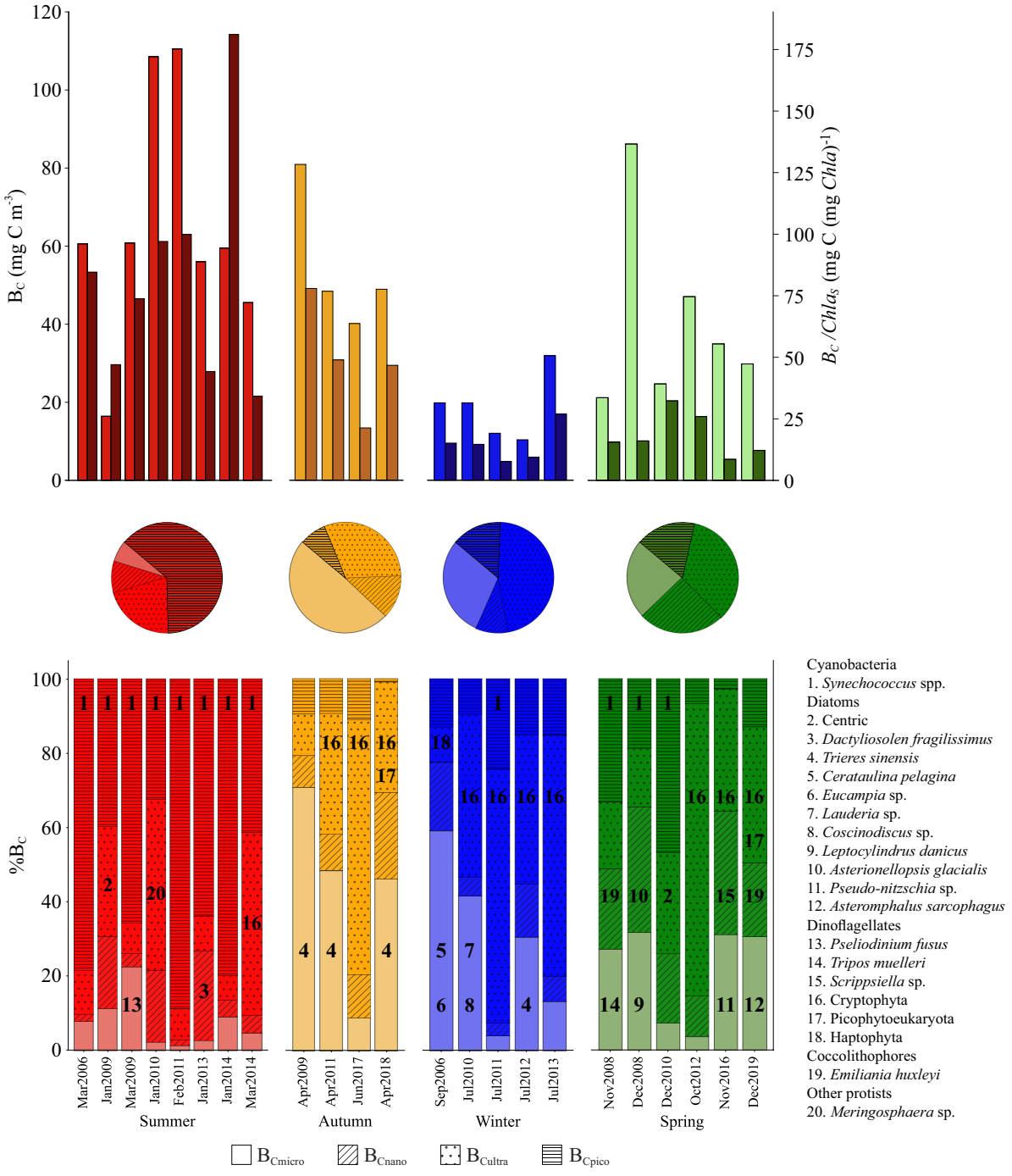

Figure 5. Top panel: bar plots showing phytoplankton carbon biomass (B_C, left y-axis, lighter bars) and the $B_C/Chla_S$ ratio (right y-axis, darker bars) across $EPEA_{PP}$. Middle panel: pie charts showing the average seasonal contribution (%) of each phytoplankton size fraction to B_C. Bottom panel: distribution of the size-fractioned B_C for each $EPEA_{PP}$. Dominant genera in the size-fractions that contributed more than 20% to B_C are labeled by number (1-20).

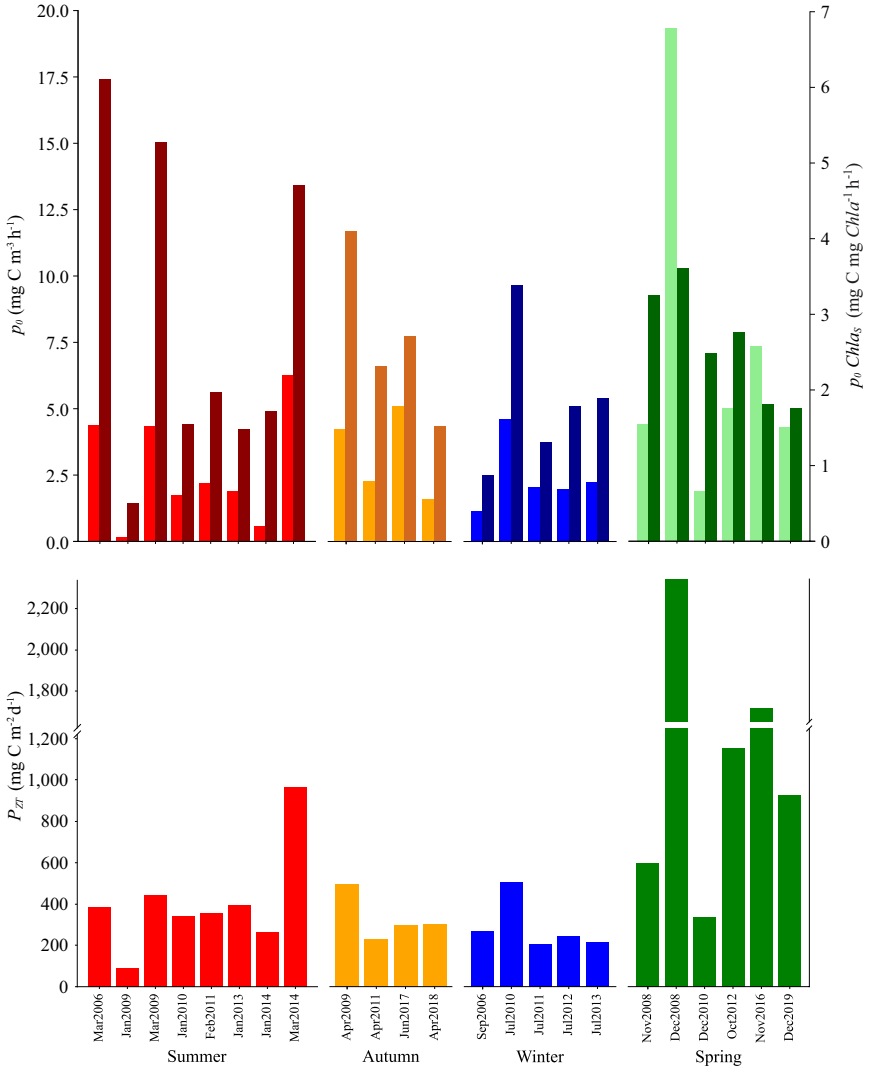

Figure 6. Top panel: bar plots showing the instantaneous primary production p_0 (bars, left y-axis) and $p_0/Chla_S$, bars, right y-axis) across $EPEA_{PP}$. Bottom panel: integrated primary production P_{ZT} during the different seasons: summer (red), autumn (orange), winter (blue) and spring (green) in the $EPEA_{PP}$.

are consistent with those previously reported for the region (Lutz et al. 2018; Segura et al. 2021). For instance, Negri (1993) documented daily productivity values between 100 and 2,700 mg C m^{-2} d^{-1} and an estimated annual PP of approximately 350 g C m^{-2} for this northern part of the Argentine shelf.

The pattern of PP observed at EPEA followed that expected for a temperate shelf marine system (Bouman et al. 2018), with maximum values occurring in spring, a period when increased solar irradiance and stratification of the water column create a favorable condition for phytoplankton growth (Sverdrup 1953; Kavanaugh et al. 2014; Franks 2015). This maximum of PP coincided with high $Chla_S$ coinciding with a well-balanced and diverse community composition that included diverse groups such as diatoms, dinoflagellates, and

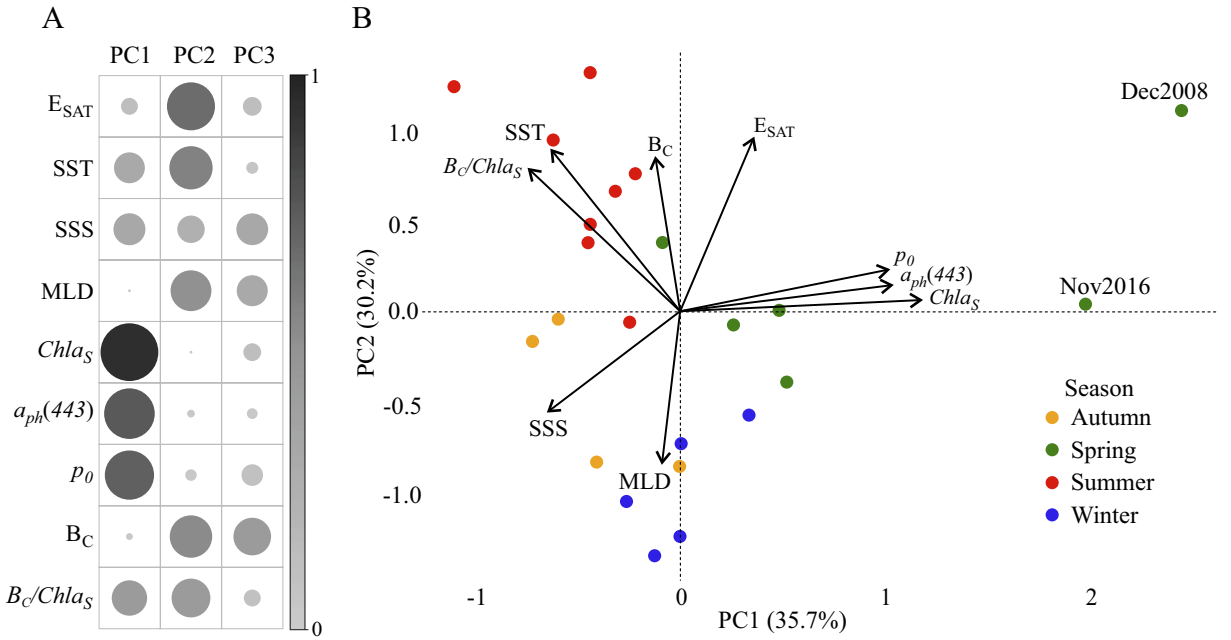

Figure 7. A) Correlation matrix diagram showing the cos² values of each variable for the first three principal components (PC1, PC2, PC3). The color bar and the dot's size indicate the correlation's strength. B) Graphical representation of the Principal Component Analysis (PCA) plot of PC1 and PC2 performed on the biological (*Chla*$_S$, $a_{ph}(443)$, p_0, B_C, $B_C/Chla_S$) and environmental (E_{SAT}, MLD, SST, SSS) variables at the sea surface. Arrows indicate the direction and strength of each variable's contribution. Each $EPEA_{PP}$ is represented by a colored circle indicating the season. Notable extreme points, such as Dec2008 and Nov2016, are labeled.

haptophytes. This aligns with bloom conditions where diverse niches coexist before resource depletion (Margalef 1978). Notably, the exceptionally high PP in Dec2008 was associated with the intrusion of waters rich in nitrate, driven by persistent southwesterly winds. This resulted in negative temperature anomalies (~ 2 °C) and positive salinity anomalies (Negri et al. 2010; Ruiz et al. 2020). The maximum PP observed in Nov2016 coincided with the presence of shelf water with lower SST and SSS relative to seasonal historical averages, and high nutrient concentrations (N + N ~ 2.00 µmol kg^{-1}). This event could have been caused by the wind-driven mixing, resulting in a deeper MLD. In contrast, low PP in spring was recorded in Dec2010, under conditions of low light availability, elevated SST, and nutrient depletion (N + N = 0.15 µmol kg^{-1}), coinciding with an unusually high proportion of *Synechococcus* spp., reflecting the high variability of the EPEA system. In summer, PP was moderate on average, and less than half of the spring values. The phytoplankton community was dominated by *Synechococcus* spp., an important component of the EPEA during this season (Lutz et al. 2006; Silva et al. 2009; Ruiz et al. 2025), which is adapted to conditions of high light, high temperature and strong stratification. The high $p_0/Chla_S$ ratio found is typical of the increased photosynthetic efficiency in small phytoplankton (Geider 1987). Furthermore, the high $B_C/Chla_S$ ratios observed are to be expected in a period when photoacclimation to high irradiance tends to decrease the intracellular *Chla*. Additionally, low nutrient availability, as observed in the $EPEA_{PP}$ and previously reported for summer at the EPEA (Ruiz et al. 2025), further contributed to the observed elevated $B_C/Chla_S$ ratios. This has implications for carbon fluxes and ecosystem functioning, since a trophic regime dominated by small

cells is associated with low export potential and a tight microbial loop (Azam and Malfatti 2007).

In autumn, PP in surface waters increased relative to summer; however, this pattern was not reflected in the depth-integrated PP values. This discrepancy could have been attributed to the higher optical clarity of the water column in summer, due to a lower absorption of optically active components (Lutz et al. 2006), thus allowing greater light penetration that favours subsurface production. Nevertheless, the ecological significance of autumn PP may be underestimated in this study due to the limited number of measurements conducted during this season, within which no events with high levels of *Chla* were encountered. It should also be noted that P_{ZT} may be biased because photosynthetic parameters were only determined at the surface. The elevated microphytoplankton biomass observed in autumn, particularly the dominance of large diatoms such as *Trieres sinensis*, is consistent with the breakdown of the thermocline and nutrient entrainment (Lutz et al. 2006, Garcia et al. 2008). These diatom blooms can contribute significantly to carbon export (Buesseler 1998).

Winter was the least productive season, primarily due to the low solar irradiance and a deep MLD that disperses phytoplankton outside the photic zone. During this period, cryptophytes of the ultraphytoplankton dominated, reflecting their ability to thrive under low-light and low-temperature conditions, as well as their mixotrophic capabilities (Stoecker et al. 2017; Lora Vilchis 2022). Large diatoms such as *Eucampia* sp., adapted to living in turbulent environments and characterized by a high nutrient affinity and uptake rates (Margalef 1978; Smayda 1997), were also abundant during this season, in agreement with previous records at EPEA (Lutz et al. 2006; Silva et al. 2009; Ruiz et al. 2025). Our results for EPEA, showing the effect on production according to different communities thriving under specific seasonal conditions, can be related to the size-dependent productivity mechanism that Fontaine et al. (2025) described for the Northeast US Shelf.

In the $EPEA_{PP}$, strong correlations were observed between α^B and E_k, as well as between α^B and environmental variables such as E_{SAT}, SST and MLD. A significant correlation was also observed between E_k and SST. In contrast, no correlation was observed between the normalized photosynthetic parameters α^B and P^Bm, nor between these and $a^B_{ph}(443)$ and $Chla_S$. These results would indicate a strong influence of the environment on the physiological properties of phytoplankton communities in this coastal environment. In addition, these results contrast with previous findings in the Argentine Sea, where photosynthetic parameters were influenced more by variations in phytoplankton community composition than by environmental factors (Lutz et al. 2010, Segura et al. 2013). Results indicate that α^B has a limited effect on the amount of carbon fixed by phytoplankton at EPEA, whereas P^Bm exerts a greater influence on primary production. Shifts in community structure may still reflect underlying environmental acclimation processes. For instance, the significant positive relationship observed between E_k and B_{Cpico} suggests an acclimation of smaller cells to higher temperatures and enhanced irradiance within stratified waters (MacIntyre et al. 2002).

Drivers of phytoplankton productivity at EPEA

In this study, PP correlated strongly with *Chla*, consistent with previous observations in other regions of the Argentine Sea (Lutz et al. 2010; Segura et al. 2013, 2021). However, no significant correlation was found between PP and B_C, which aligns with the findings of other studies on coastal ecosystems (Tiselius et al. 2016; Segura et al. 2021). This suggests that total phytoplankton carbon biomass does not always reflect their photosynthetic capacity, particularly under variable physiological or environmental conditions. The decoupling of biomass and production highlights the importance of the phytoplankton $B_C/Chla_S$ ratio as a critical link between biogeochemical models, which gen-

erally rely on carbon, and satellite-based PP models that use *Chla*. The $B_C/Chla_S$ ratio varies widely depending on taxonomic composition, cell size, and photoacclimation to light levels and nutrient availability. Consequently, natural assemblages show a broad spectrum of $B_C/Chla_S$ ratios (e.g. 20-120, Sathyendranath et al. 2020). Smaller phytoplankton tend to exhibit higher $B_C/Chla_S$ ratios, which also increase under conditions of high irradiance and nutrient limitation (Geider 1987; Sathyendranath et al. 2020; Smyth et al. 2023) (supplementary material, Figure S1). In our study, the $B_C/Chla_S$ ratio ranged from 8 to 181, indicating significant variability in how the phytoplankton responding to their environment, and was correlated positively with SST, reflecting the dominance of organisms with reduced chlorophyll content relative to carbon biomass, which is characteristic of small-sized cells acclimated to high-temperature, stratified environments. These relationships suggest that phytoplankton communities at EPEA acclimate to the summertime prevailing high-temperature, high-light conditions. However, the impact of vertical mixing on their photosynthetic traits and primary production can be challenging to identify. Despite the recognized role of the MLD in modulating both light availability and nutrient entrainment, no significant correlations were observed between MLD and the photosynthetic parameter $P^B m$ or PP rates at EPEA. One plausible explanation for this apparent decoupling lies in the dynamic nature of MLD in this coastal, wind-driven system. EPEA is subject to frequent synoptic-scale wind events that can induce rapid changes in MLD on timescales of hours to days (Carranza et al. 2018). Consequently, instantaneous MLD measurements may not accurately represent the integrated light and nutrient conditions experienced by phytoplankton communities over their growth periods. Similar observations have been reported in other coastal and shelf systems, where short-term MLD fluctuations complicate its use as a predictor of phytoplankton physiological status or productivity (Behrenfeld et al. 2013; Franks 2015). Moreover, the lag between physical forcing and biological response, particularly for traits such as photoacclimation and nutrient uptake, can obscure direct relationships in snapshot sampling (Cullen et al. 2002; Behrenfeld and Boss 2014). These findings suggest that to better assess the role of MLD as a driver of PP, it is essential to integrate physical data over biologically relevant time windows, such as growth-integrated or climatological MLD metrics (Behrenfeld and Boss 2018).

The low productivity values observed in Dec2010 and Jan2014, or high values of $Chla_S$ and PP in Dec2008 and Nov2016, may relate to phenomena of broader-scale climatic variability. Large-scale climate patterns such as the Southern Annular Mode (SAM) and the El Niño-Southern Oscillation (ENSO) are known to modulate the physical and biogeochemical dynamics of the southwestern Atlantic shelf, thereby contributing to PP variability at EPEA. The SAM phases alter atmospheric patterns on a synoptic-scale, which have been linked to enhanced stratification and reduced cross-shelf nutrient exchange in the northern Argentine shelf (Garcia et al. 2008). Similarly, ENSO variability can influence regional wind patterns, precipitation, and freshwater discharge from the Río de la Plata, which in turn affects stratification and nutrient supply to coastal systems (Piola et al. 2005; Guerrero et al. 2017). These mechanisms may alter the availability of nutrients in the euphotic zone and consequently influence PP. While no studies have directly assessed the combined or individual impacts of SAM and ENSO at EPEA, it is reasonable to hypothesize that these large-scale modes play a role in the seasonal and interannual variability observed in phytoplankton dynamics and productivity at this site (Carreto et al. 2008). To robustly evaluate this influence, sustained high-frequency sampling is needed.

While bottom-up controls such as nutrient availability, light conditions, and physical forcing are key drivers of phytoplankton variability at EPEA, top-down mechanisms, particularly zooplankton grazing, may also play a significant role in shaping

phytoplankton biomass and community composition. Zooplankton exerts selective pressure on phytoplankton, often favoring smaller, fast-growing taxa, and influencing bloom dynamics through size- and taxa-specific grazing (Calbet and Landry 2004). The seasonal dominance of large microphytoplankton forms, such as *Trieres sinensis* in autumn, could reflect periods of reduced grazing pressure or temporal mismatches between zooplankton population dynamics and phytoplankton growth. Although zooplankton abundance and phytoplankton community composition data are collected at EPEA (Silva et al. 2009; Viñas et al. 2021), these datasets have not yet been jointly analyzed to assess trophic interactions or quantify potential top-down regulation on primary producers. A future integrative analysis of these components would be crucial to better understand the role of zooplankton in modulating seasonal and interannual productivity patterns in this coastal system, particularly under the influence of climate variability (Ratnarajah et al. 2023; Jan et al. 2024).

CONCLUSIONS

This study provides the first estimates of primary production at the coastal site EPEA, with an annual average of 202 ± 115 g C m^{-2} yr^{-1}. These carbon-based estimates are essential for evaluating the carrying capacity of the system. While phytoplankton biomass is commonly estimated using chlorophyll *a* concentration due to the simplicity of analysis, our results show that the ratio $B_C/Chla_S$ has a wide range of variability at EPEA, due to changes in phytoplankton composition and physiological state. Primary production at EPEA was seasonally pulsed, modulated by variations in light, stratification, and phytoplankton composition: in line with classical and contemporary models of coastal ocean productivity (Cullen et al. 2002; Behrenfeld and Boss 2018). However, observed deviations from expected seasonal patterns highlight the sensitivity of coastal PP to both local and remote forcing. The results presented in this study provide valuable insight into the seasonal and interannual variability of PP, photosynthetic parameters, and phytoplankton physiology conditions at EPEA. Our findings highlight the physiological plasticity of phytoplankton communities in response to heterogeneous environmental conditions in coastal systems. This knowledge is essential for improving PP models, particularly in the under-sampled Argentine continental shelf.

Integrating physiological, ecological, and physical data will enhance understanding of ecosystem productivity at EPEA and provide insights into its potential resilience to ongoing environmental change. Moreover, increasing the frequency of PP determinations at this site will improve our ability to characterize temporal variability and refine primary productivity models, ultimately aiding in the development of robust regional forecasts.

ACKNOWLEDGEMENTS

We are thankful to all the colleagues at the 'Dinámica del Plancton Marino y Cambio Climático' program, as well as other programs from the Instituto Nacional de Investigación y Desarrollo Pesquero (INIDEP) and the Servicio de Hidrografía Naval (SHN) for the invaluable collaboration on board. This work was financed by INIDEP and by the 'Agencia Nacional de Promoción Científica y Tecnológica' project PICT19-2178. This is INIDEP contribution no 2463.

Author contributions

Valeria Segura: conceptualization; methodology; software; formal analysis; investigation; data curation; writing-original draft; writing-review and editing; visualization; project administration. Daniela Del Valle: conceptualization; formal analysis;

investigation; writing-original draft; writing-review and editing. Vivian A. Lutz: conceptualization; methodology; investigation; writing-review and editing; supervision; funding acquisition; project administration. Moira Luz Clara: formal analysis; investigation; data curation; writing-review and editing. Ricardo I. Silva: investigation; formal analysis; software; data curation. Jorge Fernández Acuña: formal analysis; methodology; data curation; visualization. M. Guillermina Ruiz: investigation; formal analysis; data curation. Lucrecia Allega: investigation; formal analysis; visualization. Carla F. Berghoff: investigation; formal analysis; methodology; software; data curation. Guillermina García Facal: investigation; formal analysis; visualization. Lucia Epherra: investigation; formal analysis; visualization.

REFERENCES

Armstrong FAJ, Stearns CA, Strickland JDH. 1967. The measurement of upwelling and subsequent biological processes by means of the Technicon Autoanalyzer and associated equipment. Deep Sea Res. 14: 381-389.

Azam F, Malfatti F. 2007. Microbial structuring of marine ecosystems. Nat Rev Microbiol. 5 (10): 782-791.

Baldoni A, Molinari G, Guerrero RA, Kruk M. 2008. Base regional de datos oceanográficos (BaRDO) INIDEP. Inf Invest INIDEP Nº 13/2008. 25 p.

Balech E. 1988. Los dinoflagelados del Atlántico Sudoccidental. Publicaciones Especiales. Instituto Español de Oceanografía. 1. 310 p.

Behrenfeld MJ, Boss ES. 2014. Resurrecting the ecological underpinnings of ocean plankton blooms. Ann Rev Mar Sci. 6 (1): 167-194.

Behrenfeld MJ, Boss ES. 2018. Student's tutorial on bloom hypotheses in the context of phytoplankton annual cycles. Glob Chang Biol. 24 (1): 55-77.

Behrenfeld MJ, Hu Y, Hostetler CA, Dall'Olmo G, Rodier SD, Hair JW, Trepte CR. 2013. Space-based lidar measurements of global ocean carbon stocks. Geophys Res Lett. 40 (16): 4355-4360.

Booth BC. 1993. Estimating cell concentration and biomass of autotrophic plankton using microscopy. In: Kemp PF, Sherr BF, Sherr EB, Cole JJ, editors. Handbook of methods in aquatic microbial ecology. Boca Raton: Lewis Publishers. p. 199-205.

Bouman H, Platt T, Sathyendranath S, Stuart V. 2005. Dependence of light-saturated photosynthesis on temperature and community structure. Deep Sea Res 1 Oceanogr Res Pap. 52 (7): 1284-1299.

Bouman HA, Platt T, Doblin M, Figueiras FG, Gudmundsson K, Gudfinnsson HG, Huang B, Hickman A, Hiscock M, Jackson T. 2018. Photosynthesis-irradiance parameters of marine phytoplankton: synthesis of a global data set. Earth Syst Sci Data. 10 (1): 251-266.

Buesseler KO. 1998. The decoupling of production and particulate export in the surface ocean. Global Biogeochem Cycles. 12 (2): 297-310.

Buratti CC, Chidichimo MP, Cortés F, Gaviola S, Martos P, Prosdocimi L, Seitune D, Verón E. 2022. Estado del conocimiento de los efectos del cambio climático en el Océano Atlántico Sudoccidental sobre los recursos pesqueros y sus implicancias para el manejo sostenible. Buenos Aires: Ministerio de Agricultura, Ganadería y Pesca. 225 p.

Calbet A, Landry MR. 2004. Phytoplankton growth, microzooplankton grazing, and carbon cycling in marine systems. Limnol Oceanogr. 49 (1): 51-57.

Carranza MM, Gille ST, Franks PJ, Johnson KS, Pinkel R, Girton JB. 2018. When mixed layers are not mixed. Storm-driven mixing and bio-optical vertical gradients in mixed layers of the Southern Ocean. J Geophys Res Oceans. 123 (10): 7264-7289.

Carreto JI, Lutz VA, Carignan MO, Colleoni

ADC, De Marco SG. 1995. Hydrography and chlorophyll *a* in a transect from the coast to the shelf-break in the Argentinian Sea. Cont Shelf Res. 15 (2-3): 315-336.

Carreto JI, Montoya NG, Akselman R, Negri RM, Carignan MO, Cucchi Colleoni A. 2004. Differences in the PSP toxin profiles of *Mytilus edulis* during spring and autumn blooms of *Alexandrium tamarense* off Mar del Plata coast, Argentina. In: Steidinger KA, Landsberg J, Tomas CR, Vargo GA, editors. Harmful algae 2002 Florida Fish and Wildlife Conservation Commission, Florida Institute of Oceanography, and Intergovernmental Oceanographic Commission of UNESCO. p. 100-102.

Carreto JI, Montoya NG, Akselman R, Carignan MO, Silva RI, Colleoni DAC. 2008. Algal pigment patterns and phytoplankton assemblages in different water masses of the Río de la Plata maritime front. Cont Shelf Res. 28 (13): 1589-1606.

Collos Y, Slawyk G. 1985. On the compatibility of carbon uptake rates calculated from stable and radioactive isotope data: implications for the design of experimental protocols in aquatic primary productivity. J Plankton Res. 7 (5): 595-603.

Cullen JJ, Franks PJ, Karl DM, Longhurst A. 2002. Physical influences on marine ecosystem dynamics. In: Robinson AR, McCarthy JJ, Rothschild BJ, editors. Biological-physical interactions in the sea. New York: Wiley. p. 297-336.

Cupp EE. 1943. Marine plankton diatoms of the west coast of North America. Bull Scripps Inst Oceanogr. 5 (1): 1-238.

de Boyer Montégut C, Madec G, Fischer AS, Lazar A, Iudicone D. 2004. Mixed layer depth over the global ocean: an examination of profile data and a profile-based climatology. J Geophys Res Oceans. 109: 12003.

Dogliotti AI, Lutz VA, Segura V. 2014. Estimation of primary production in the southern Argentine continental shelf and shelf-break regions using field and remote sensing data. Remote Sens Environ. 140: 497-508.

Dubinsky Z, Falkowski PG, Wyman K. 1986. Light harvesting and utilization by phytoplankton. Plant Cell Physiol. 27 (7): 1335-1349.

Edwards M, Beaugrand G, Hays GC, Koslow JA, Richardson A. 2010. Multi-decadal oceanic ecological datasets and their application in marine policy and management. Trends Ecol Evol. 25 (10): 602-610.

Falkowski PG. 1980. Light-shade adaptation in marine phytoplankton. In: Falkowski PG, editor. Primary productivity in the sea. New York: Plenum Press. p. 99-119.

Falkowski PG. 2002. On the evolution of the carbon cycle. In: Williams PJ, Thomas DN, Reynolds CS, editors. Phytoplankton productivity - carbon assimilation in marine freshwater ecosystems. Blackwell. p. 318-349.

Falkowski PG. 2012. The power of plankton: Do tiny floating microorganisms in the ocean's surface waters play a massive role in controlling the global climate? Nature. 483 (7387): 17-20.

Falkowski PG, Laws EA, Barber RT, Murray JW. 2003. Phytoplankton and their role in primary, new, and export production. In: Fasham MJR, editor. Ocean biogeochemistry: the role of the ocean carbon cycle in global change. Global Change - The IGBP Series. Springer. p. 99-121.

Fernández IC, Raimbault P, Garcia N, Rimmelin P, Caniaux G. 2005. An estimation of annual new production and carbon fluxes in the northeast Atlantic Ocean during 2001. J Geophys Res Oceans. 110 (C7).

Fontaine DN, Marrec P, Menden-Deuer S, Sosik HM, Rynearson TA. 2025. Time series of phytoplankton net primary production reveals intense interannual variability and size-dependent chlorophyll-specific productivity on a continental shelf. Limnol Oceanogr. 70: 203-216.

Franco BC, Palma ED, Combes V, Lasta M L. 2017. Physical processes controlling passive larval transport at the Patagonian Shelf Break

Front. J Sea Res. 124: 17-25.

Franks PJS. 2015. Has sverdrup's critical depth hypothesis been tested? Mixed layers vs. turbulent layers. ICES J Mar Sci. 72 (6): 1897-1907.

Frouin R, Pinker R. 1995. Estimating photosynthetically active radiation (PAR) at the earth's surface from satellite observations. Remote Sens Environ. 51 (1): 98-107.

Garcia VM, Garcia CA, Mata MM, Pollery RC, Piola AR, Signorini SR, McClain CR, Iglesias-Rodriguez MD. 2008. Environmental factors controlling the phytoplankton blooms at the Patagonia shelf-break in spring. Deep Sea Res 1 Oceanogr Res Pap. 55 (9): 1150-1166.

Geider RJ. 1987. Light and temperature dependence of the carbon to chlorophyll *a* ratio in microalgae and cyanobacteria: Implications for physiology and growth of phytoplankton. New Phytol. 106 (1): 1-34.

Grasshoff K, Kremling K, Ehrhardt M. 1983. Determination of nutrients. In methods of seawater analysis. 2nd ed. Weinheim: WileyVCH.

Guerrero RA, Piola AR. 1997. Masas de agua en la plataforma continental. In: Boschi E, editor. El Mar Argentino y sus recursos pesqueros. Tomo 1. Antecedentes históricos de las exploraciones en el mar y las características ambientales. Mar del Plata: Instituto Nacional de Investigacion y Desarrollo Pesquero. p. 107-118.

Guiry MD, Guiry GM. 2025. AlgaeBase. Worldwide electronic publication. University of Galway. [accessed 2025 Oct 21]. https://www.algaebase.org.

Hama T, Miyazaki T, Ogawa Y, Iwakuma T, Takahashi M, Otsuki A, Ichimura S. 1983. Measurement of photosynthetic production of a marine phytoplankton population using a stable 13C isotope. Mar Biol. 73 (1): 31-36.

Hillebrand H, Dürselen C-D, Kirschtel D, Pollingher U, Zohary T. 1999. Biovolume calculation for pelagic and benthic microalgae. J Phycol. 35 (2): 403-424.

Hoepffner N, Sathyendranath S. 1992. Bio-optical characteristics of coastal waters: absorption spectra of phytoplankton and pigment distribution in the western North Atlantic. Limnol Oceanogr. 37 (8): 1660-1679.

Holm-Hansen O, Lorenzen CJ, Holmes RW, Strickland JD. 1965. Fluorometric determination of chlorophyll. ICES J Mar Sci. 30 (1): 3-15.

IPCC 2019. IPCC Special report on the ocean and cryosphere in a changing climate. [accessed 2025 Oct 21]. https://www.ipcc.ch/srocc/.

Jan KM, Serandour B, Walve J, Winder M. 2024. Plankton blooms over the annual cycle shape trophic interactions under climate change. Limnol Oceanogr Lett. 9 (3): 209-218.

Karlson B, Godhe A, Cusack C, Bresnan E. 2010. Introduction to methods for quantitative phytoplankton analysis. In: Karlson B, Cusack C, Bresnan E, editors. Microscopic and molecular methods for quantitative phytoplankton analysis. UNESCO. p. 5-20.

Kavanaugh MT, Hales B, Saraceno M, Spitz YH, White AE, Letelier RM. 2014. Hierarchical and dynamic seascapes: a quantitative framework for scaling pelagic biogeochemistry and ecology. Prog Oceanogr. 120: 291-304.

Kulk G, Platt T, Dingle J, Jackson T, Jönsson BF, Bouman HA, Babin M, Brewin RJ, Doblin M, Estrada M. 2020. Primary production, an index of climate change in the ocean: Satellite-based estimates over two decades. Remote Sens Environ. 12 (5): 826.

Lê S, Josse J, Husson F. 2008. Factominer: An R package for multivariate analysis. J Stat Softw. 25: 1-18.

Longhurst A, Sathyendranath S, Platt T, Caverhill C. 1995. An estimate of global primary production in the ocean from satellite radiometer data. J Plankton Res. 17 (6): 1245-1271.

Lora Vilchis MC. 2022. Cryptophyte: biology, culture, and biotechnological applications. In: Queiroz Zepka L, Jacob-Lopes E, Deprá MC, editors. Progress in microalgae research - a path for shaping sustainable futures. Rijeka: IntechOpen. p. 17-40.

Lucas AJ, Guerrero RA, Mianzán HW, Acha EM, Lasta CA. 2005. Coastal oceanographic regimes of the Northern Argentine Continental Shelf (34-43° S). Estuar Coast Shelf Sci. 65 (3): 405-420.

Lund JWG, Kipling C, Le Cren E. 1958. The inverted microscope method of estimating algal numbers and the statistical basis of estimations by counting. Hydrobiologia. 11 (2): 143-170.

Lutz VA, Ruiz MG, Segura V. 2021. Protocolo para la determinación del coeficiente de absorción espectral de la luz por el material particulado (total, no-algal y fitoplancton) en agua de mar. Inf Proc Operc INIDEP Nº 3/2021. 10 p.

Lutz VA, Segura V, Dogliotti AI, Gagliardini DA, Bianchi AA, Balestrini CF. 2010. Primary production in the Argentine Sea during spring estimated by field and satellite models. J Plankton Res. 32 (2): 181-195.

Lutz VA, Segura V, Dogliotti A, Tavano V, Brandini FP, Calliari DL, Ciotti AM, Villafañe VF, Schloss IR, Corrêa FMS. 2018. Overview on primary production in the Southwestern Atlantic. In: Hoffmeyer M, Sabatini M, Brandini F, Calliari D, Santinelli N, editors. Plankton ecology of the Southwestern Atlantic: from the subtropical to the subantarctic realm. Springer. p. 101-126.

Lutz VA, Subramaniam A, Negri RM, Silva RI, Carreto JI. 2006. Annual variations in bio-optical properties at the 'Estación Permanente de Estudios Ambientales (EPEA)' coastal station, Argentina. Cont Shelf Res. 26 (10): 1093-1112.

MacIntyre HL, Kana TM, Anning T, Geider RJ. 2002. Photoacclimation of photosynthesis irradiance response curves and photosynthetic pigments in microalgae and cyanobacteria. J Phycol. 38 (1): 17-38.

Margalef R. 1978. Life-forms of phytoplankton as survival alternatives in an unstable environment. Oceanol Acta. 1 (4): 493-509.

Menden-Deuer S, Lessard EJ. 2000. Carbon to volume relationships for dinoflagellates, diatoms, and other protist plankton. Limnol Oceanogr. 45 (3): 569-579.

Mitchell BG. 1990. Algorithms for determining the absorption coefficient for aquatic particulates using the quantitative filter technique. Proc Ocean Optics X. 1302: 137-148.

Murphy J, Riley JP. 1962. A modified single solution method for the determination of phosphate in natural waters. Anal Chim Acta. 27: 31-36.

Negri R. 1993. Seminario taller sobre la dinámica marina y su impacto en la productividad de las regiones frontales del Mar Argentino. INIDEP Inf Téc. 1. 7 p.

Negri R, Akselman R, Carignan M, Cucchi Colleoni A, Díaz M, Diovisalvi N, Hozbor C, Leonarduzzi E, Lutz V, Molinari G. 2010. Plankton community and environmental conditions during a mid-shelf waters intrusion and upwelling at the EPEA station (Argentina). Meeting of the Americas AGU, Foz do Iguazu, Brazil. p. 8-10.

Nixon SW. 1995. Coastal marine eutrophication: a definition, social causes, and future concerns. Ophelia. 41 (1): 199-219.

O'Brien TD, Lorenzoni L, Isensee K, Valdés L. 2017. What are marine ecological time series telling us about the ocean? A status report. IOC-UNESCO, IOC Technical Series. 129. 297 p.

Piola AR, Matano RP, Palma ED, Möller Jr. OO, Campos EJD. 2005. The influence of the Plata River discharge on the western South Atlantic shelf. Geophys Res Lett. 32 (1): L01603.

Platt T, Gallegos CL. 1980. Modelling primary production. In: Falkowski PG, editor. Primary productivity in the sea. Boston: Springer. p. 339-362.

Platt T, Gallegos CL, Harrison WG. 1980. Photoinhibition of photosynthesis in natural assemblages of marine phytoplankton. J Mar Res. 38 (4): 687-701.

Platt T, Sathyendranath S. 1988. Oceanic primary production: estimation by remote sensing at local and regional scales. Science. 241 (4873): 1613-1620.

Platt T, Sathyendranath S, Ulloa O, Harrison WG, Hoepffner N, Goes J. 1992. Nutrient control of phytoplankton photosynthesis in the western North Atlantic. Nature. 356 (6366): 229-231.

R Core Team. 2024. R: A Language and Environment for Statistical Computing. R Foundation for Statistical Computing. https://www.R-project.org/.

Ratnarajah L, Abu-Alhaija R, Atkinson A, Batten S, Bax NJ, Bernard KS, Canonico G, Cornils A, Everett JD, Grigoratou M. 2023. Monitoring and modelling marine zooplankton in a changing climate. Nat Commun. 14 (1): 564.

Ruiz MG. 2018. Variabilidad de las propieades bio-ópticas en la serie de tiempo Estación Permanente de Estudios Ambientales (EPEA) complementando mediciones in situ y satelitales [PhD thesis]. Mar del Plata: Facultad de Ciencias Exactas y Naturales, Universidad Nacional de Mar del Plata. 137 p.

Ruiz MG, Coy MBM, Carignan MC, Albornoz M, Molinari GN, Montoya NG. 2025. Seasonal variability of phytoplankton community structure in a coastal station of the Argentine continental shelf based on a chemotaxonomic approach. Mar Fish Sci. 38 (1): 61-83.

Ruiz MG, Lutz VA, Segura V, Berghoff CF, Negri R. 2020. The color of EPEA: variability in the *in situ* bio-optical properties in the period 2000-2017. Mar Fish Sci. 33 (2): 205-225.

Sathyendranath S, Lazzara L, Prieur L. 1987. Variations in the spectral values of specific absorption of phytoplankton. Limnol Oceanogr. 32 (2): 403-415.

Sathyendranath S, Platt T. 1988. The spectral irradiance field at the surface and in the interior of the ocean: a model for applications in oceanography and remote sensing. J Geophys Res Oceans. 93 (C8): 9270-9280.

Sathyendranath S, Platt T, Kovač Ž, Dingle J, Jackson T, Brewin RJ, Franks P, Marañón E, Kulk G, Bouman HA. 2020. Reconciling models of primary production and photoacclimation. Appl Opt. 59 (10): 100-114.

Segura V. 2013. Variaciones en la producción primaria en relación con los distintos tipos funcionales del fitoplancton en el Mar Argentino [PhD thesis]. Mar del Plata: Facultad de Ciencias Exactas y Naturales, Universidad Nacional de Mar del Plata. 139 p.

Segura V, Lutz VA, Dogliotti A, Silva RI, Negri RM, Akselman R, Benavides H. 2013. Phytoplankton types and primary production in the Argentine Sea. Mar Ecol Prog Ser. 491: 15-31.

Segura V, Silva RI, Clara ML, Martos P, Cozzolino E, Lutz VA. 2021. Primary production and plankton assemblages in the fisheries ground around San Jorge Gulf (Patagonia) during spring and summer. Plankton Benthos Res. 16 (1): 24-39.

Silva R, Negri R, Lutz V. 2009. Summer succession of ultraphytoplankton at the EPEA coastal station (Northern Argentina). J Plankton Res. 31 (4): 447-458.

Smayda TJ. 1997. Harmful algal blooms: their ecophysiology and general relevance to phytoplankton blooms in the sea. Limnol Oceanog. 42 (5 part 2): 1137-1153.

Smyth T, Moffat D, Tarran G, Sathyendranath S, Ribalet F, Casey J. 2023. Determining drivers of phytoplankton carbon to chlorophyll ratio at Atlantic Basin scale. Front Mar Sci. 10: 1191216.

Stoecker DK, Hansen PJ, Caron DA, Mitra A. 2017. Mixotrophy in the marine plankton. Ann Rev Mar Sci. 9 (1): 311-335.

Sverdrup HU. 1953. On conditions for the vernal blooming of phytoplankton. J Cons. 18 (3): 287-295.

Tiselius P, Belgrano A, Andersson L, Lindahl O. 2016. Primary productivity in a coastal ecosystem: a trophic perspective on a long-term time series. J Plankton Res. 38 (4): 1092-1102.

Tomas CR. 1997. Identifying marine phytoplankton. Cambridge: Elsevier.

Valdés L, Lomas M. 2017. New light for ship-based time series. In: O'Brien TD, Lorenzoni L, Isensee K, Valdés L, editors. What are Marine Ecological Time Series telling us about the ocean. A status report. IOC UNESCO, IOC Technical Series. 129. p. 11-17.

Veritiy PG, Sieracki ME. 1993. Use of color image analysis and epifluorescence microscopy to measure plankton biomass. In: Kemp PF, Sherr BF, Sherr EB, Cole JJ, editors. Handbook of methodology in aquatic microbial ecology. Boca Raton: Lewis Publishers. p. 187-197.

Viñas MD, Cepeda GD, Clara ML. 2021. Linking long-term changes of the zooplankton community to the environmental variability at the EPEA station (southwestern Atlantic Ocean). Mar Fish Sci. 34 (2): 211-234.

Volk T, Hoffert MI. 1985. Ocean carbon pumps: analysis of relative strengths and efficiencies in ocean-driven atmospheric CO_2 changes. In: Sundquist ET, Broecker WS, editors. The carbon cycle and atmospheric CO_2: natural variations archean to present. Geophysical Monograph. Vol. 32. Washington: AGU. p. 99-110.

Young JR, Bown PR, Lees JA. 2022. Nannotax3 website. International Nannoplankton Association. [accessed 2022 Apr 21]. https://www.mikrotax.org/Nannotax3.